Atmospheric Circulation Influenced by the Oceanic Subtropical Front in the North Pacific

Fumiaki Kobashi[1], Shang-Ping Xie[2], Naoto Iwasaka[1], and Takashi T. Sakamoto[3]

[1]Faculty of Marine Technology, Tokyo University of Marine Science and Technology, Japan

[2]International Pacific Research Center and Department of Meteorology, University of Hawaii, USA

[3]Frontier Research Center for Global Change, Japan Agency for Marine-Earth Science and Technology, Japan

Correspondence: kobashi@kaiyodai.ac.jp

INTRODUCTION

Surface wind fields over the subtropical North Pacific are characterized by anticyclonic vorticity with the westerlies to the north and the northeast trade winds to the south. The anticyclonic wind stress curls drive the basin-scale subtropical gyre. About 40 years ago, Yoshida and Kidokoro (1967a, b) found a weak local minimum of anticyclonic vorticity in the midst of the subtropical gyre, based on an analysis of seasonal-mean wind stress computed by Hidaka (1958). They suggested that this trough of anticyclonic wind curls produces an eastward current called the Subtropical countercurrent (STCC), which was just discovered by Uda and Hasunuma (1969) from direct current meter measurements and geostrophic calculations.

Many studies of the formation mechanisms for STCC have followed. Using an ocean general circulation model (GCM), Takeuchi (1984) produced an STCC using wind stress forcing without the wind curl trough, indicating that the wind curl trough of Yoshida and Kidokoro (1967a, b) is not essential for the STCC. Recent theoretical (Kubokawa 1999) and numerical (Kubokawa and Inui 1999) studies showed that the STCC is associated with distinct potential vorticity structures caused by the circulation of mode waters in the ventilated thermocline, a mechanism that has won support from observations (Aoki et al. 2002; Kobashi et al. 2006). This mechanism does not require an anticyclonic curl trough but generates an STCC with smooth wind forcing.

There are no follow-up studies since Yoshida and Kidokoro (1967a, b) to re-examine the wind curl trough they reported. It is unclear whether their wind curl trough is a robust feature of the subtropical gyre or an artifact of noisy data of Hidaka (1958). The present paper examines surface wind fields over the subtropical Northwest Pacific using the QuikSCAT vector wind observations that have accumulated since 1999. Our results confirm the wind curl trough of Yoshida and Kidokoro (1967a, b) and show that the wind curls near the STCC even turn cyclonic during spring. We then proceed to study the three-dimensional structure of the atmosphere and processes that lead to the formation of these cyclonic wind curls in the subtropical gyre, using an atmospheric reanalysis product. We show that the atmospheric response to the STF has a deep vertical structure, distinct from that near other SST fronts over the cool ocean as reviewed in Xie (2004).

DATA

This study uses surface vector wind velocity measured by the QuikSCAT scatterometer, sea surface temperature (SST), columnar water vapor, and precipitation by the Tropical Rainfall Measuring Mission (TRMM) satellite's Microwave Imager (TMI), from August 1999 to December 2006. Both products are processed by Remote Sensing Systems onto 3-day running mean maps on a 0.25º grid. We compute wind stress based on drag coefficients of Kondo (1975), and calculate the curl by applying a spatial running mean with 1º latitude and 3º longitudes in order to extract large-scale vorticity structure.

We use the Japanese 25-year Reanalysis (JRA-25; Onogi et al. 2007), which is produced jointly by the Japan Meteorological Agency (JMA) and Central Research Institute of Electric Power Industry (CRIEPI). This study

uses 6-hourly fields of air temperature, specific humidity, horizontal and vertical velocities available on a 1.25º grid and at 12 vertical levels from 1000 hPa to 100 hPa. 6-hourly surface variables (wind velocity and stress vectors, air temperature, specific humidity, sea level pressure, and precipitation rate) are available on the T106 Gaussian grid. Our analysis covers the period of January 2000 to December 2006.

RESULTS

Figure 1 shows the May climatology of SST, wind stress curl, and columnar water vapor, all derived from satellite. The STF is clearly identified with a zone of large SST gradients between 20º and 30ºN. The wind stress curl is generally anticyclonic (negative) over the subtropical region, but there is a band of a local minimum in anticyclonic curls with some narrow cyclonic (positive) curls between 22º and 28ºN west of about 155ºE. The anticyclonic curl trough is approximately collocated with the STF. The columnar water vapor map features a tongue-like band of high columnar water vapor that extends eastward up to 155ºE between 18º and 26ºN. This high-moisture band is located in the area of high SST above 27ºC and is slightly displaced south of the wind curl trough and the STF, suggesting a deep vertical structure of the STF's influence on the atmosphere.

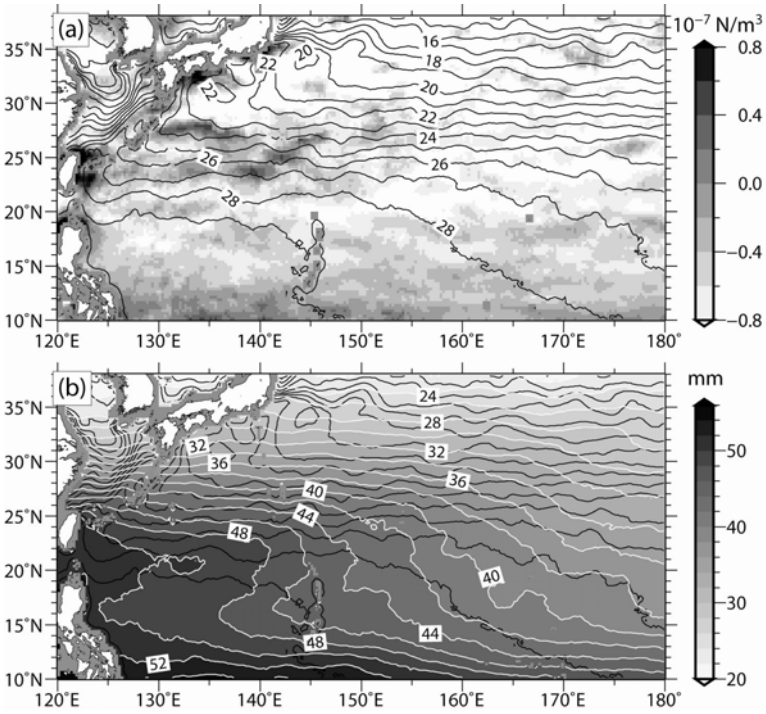

Figure 1: May climatology from satellite observations: (a) wind stress curl and (d) columnar water vapor, along with SST in contours.

The wind curl trough exhibits a clear seasonality. Although the subtropical region is overall occupied by anticyclonic curls throughout the year, the anticyclonic curl decreases in the STF region from April to May, with a pronounced meridional minimum in May. This curl trough is coincident with the seasonal intensification of the SST gradient in the STF from April and May. It is also found that the wind curl trough during April-May is coincident with the abrupt increase in columnar water vapor that is related to the formation of the high-moisture tongue. These results from satellite observations are confirmed from the JRA-25 data.

The cyclonic curl in the STF region appears different from the prevalent wind adjustment to SST fronts elsewhere as reviewed in Xie (2004). A vertical mixing mechanism (Wallace et al. 1989) is considered important in the latter type of atmospheric adjustment as observed along the Kuroshio and its extension. In this mechanism, an increase in SST reduces the static stability of the near-surface atmosphere and intensifies the vertical mixing,

bringing fast-moving air aloft down to the sea surface and accelerating the surface wind. Thus, surface winds blowing parallel to the SST front are accelerated and decelerated on the warm and cold sides of the SST front, respectively. Over the STF region, however, the prevailing winds are easterly. The wind adjustment by the vertical mixing mechanism would accelerate (decelerate) the easterlies on the southern (northern) flank of the SST front, generating an anticyclonic wind curl, opposite to what is observed. Some other mechanisms are responsible for the cyclonic wind curl along the STF.

Spatio-temporal characteristics of the wind curl trough are examined using JRA-25. The time-longitude diagrams of surface wind curl, surface pressure and rain rate indicate that in the STF region, cyclonic wind curls occur intermittently and propagate eastward with a typical period of several days. The cyclonic curl is accompanied by rain and low sea level pressure, suggesting a deep structure in the atmosphere. Indeed JRA-25 indicates that precipitation in this region is due largely to convective precipitation rather than large-scale condensation.

The vertical structure of the cyclonic wind curl is investigated using JRA-25. For this, we make two composites based on the 7-year May time series of wind curl meridionally averaged between 23º and 27ºN at 142.875ºE: one by averaging the data when positive curl values exceed one standard deviation, and one by averaging the data when the curl is negative. Note that our results are not sensitive to the choice of the reference longitude; the same results are obtained at other nearby longitudes. Out of 868 6-hourly maps, 81 and 493 go into the strong cyclonic and anticyclonic curl composites, respectively.

In both composites, the meridional variations in surface air temperature (SAT) follow well those in SST, and an air temperature front is anchored by the STF between 21º and 29ºN within the atmospheric boundary layer below 925 hPa. Thus, the STF maintains surface baroclinicity of the atmosphere. It is noted that the temperature front is also recognized as the front of equivalent potential temperature, because of the contrast between warm and wet air to the south and cold and dry air to the north.

Although there is no notable difference in SST, the distributions of wind and temperature are quite different between the two composites. When the cyclonic curl is absent at the surface, southerly winds are dominant at the surface in the STF region. On the other hand, when the cyclonic curl is present, northerly winds blow from the north onto the STF and converge with the southerly winds, leading to a strong upward motion around 24ºN. The upward motion is consistent with the result that the cyclonic curl is associated with low sea level pressure. The SAT decreases (increases) significantly north (south) of the wind convergence as a result of cold (warm) advection in the boundary layer.

Figure 2 shows the cyclonic-anticyclonic composite difference. The surface wind convergence near the STF is caused by both the northerly winds and the intensified southerly winds. The upward motion occurs mainly over the southern, warm flank of the STF between 21º and 26ºN and reaches up to the 200 hPa level with a maximum upward velocity of 2.6 cm/s around the 300 hPa level, causing large changes in the circulation of the upper troposphere. The upward motion is coincident with significant increase in moisture, especially in the lower troposphere (Figs. 2b), and a local maximum in convective rain (Figs. 2c). Another remarkable feature for the cyclonic curl is the presence of a downward motion to the north of 30ºN below 200 hPa, accompanied by the decrease in tropospheric moisture and convective rain.

The increase in moisture occurs over the entire air column between 21º and 26ºN because of the moisture supply by the upward motion. Specific humidity forms a broad meridional maximum above the atmospheric boundary layer (not shown), consistent with the humid tongue in satellite-observed columnar water vapor (Fig. 1b). The latter lends strong support that the surface cyclonic curls near the STF are associated with deep atmospheric adjustments. Convective heating on the southern flank of the STF lowers surface pressure, forcing deep upward motion. The vertical stretching in the convective region causes cyclonic vorticity in the lower troposphere as observed by QuikSCAT in surface winds.

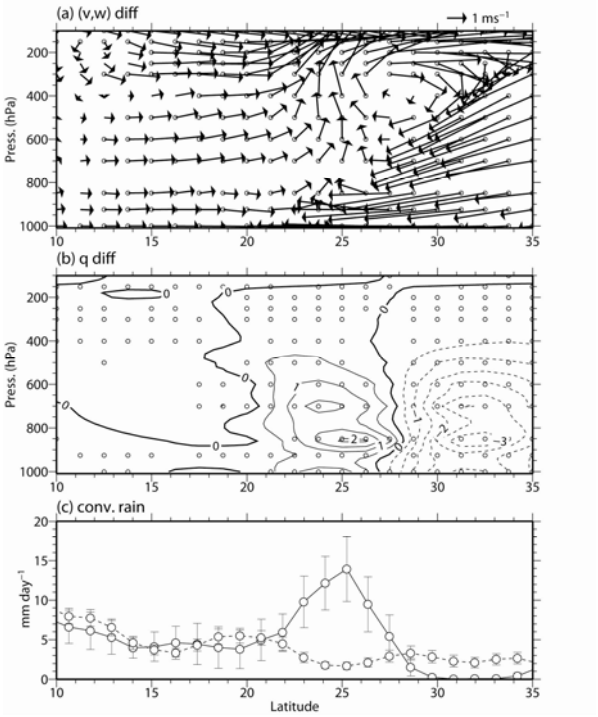

Figure 2: Cyclonic-anticyclonic curl composite differences of (a) meridional and vertical winds and (b) specific humidity (g/kg) at 142.875ºE. Open circles in (a) and (b) show grid points of significant difference with confidence greater than 95%. The vertical wind speed is multiplied by 100. (c) Convective rain rate (mm/day) in the cyclonic (solid line) and the anticyclonic (dashed line) curl composites, along with 95% confidence intervals.

The longitude-height sections of cyclonic-anticyclonic composite differences in geopotential height, vector wind velocity and potential temperature reveal that the axis of the low pressure trough associated with the cyclonic curl tilts westward with height. The upward motion occurs to the east of this trough axis where temperature mostly increases, while in the downward motion region west of the trough axis, temperature decreases. This pattern of warm air rising and cold air sinking indicates the well-known energy conversion from potential to kinetic energy. Thus, the disturbance with surface cyclonic curl is associated with atmospheric baroclinic instability over the STF.

Not only cyclonic, but also anticyclonic disturbances are found along the STF from the composite analysis. We examine the probability density function of disturbances along the STF using high-pass filtered sea level pressures. The frequency of low disturbances is generally higher than that of high disturbances, and the deviation of the Gaussian increases with negative sea level pressures relative to the baseline Gaussian distribution, indicating that low pressure systems tend to be well developed through baroclinic instability probably due to the effect of convective heating. This asymmetry of the disturbances results in the formation of the cyclonic band along the STF.

We now turn to the evolution of the disturbance that brings about cyclonic curls on the horizontal plane. We calculate lagged composite maps of wind stress curl, sea level pressure, surface wind velocity, and geopotential height at 500 hPa, with reference to cyclonic wind curl at 142.875ºE, 25ºN. The temporal high-pass filter is applied to wind velocity, sea level pressure, and geopotential height by subtracting a 15-day running mean. Figure 3 shows the surface result at no lag.

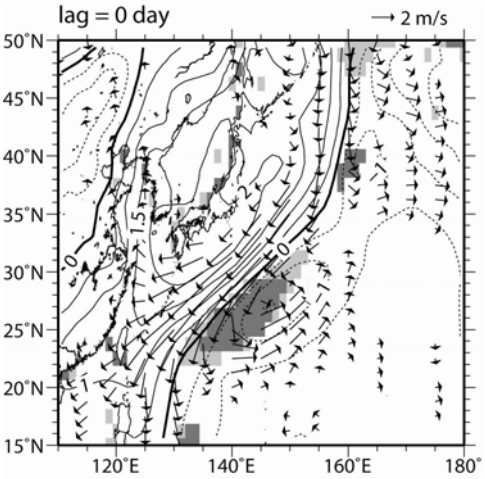

Figure 3: Composite maps of wind stress curl (shade) and temporally high-pass filtered surface wind and sea level pressure (hPa; contours), with reference to the cyclonic wind curl at 142.875ºE. Wind velocity less than 0.5 m/s is masked out. Wind stress curl is shown only for a significantly cyclonic area with 95% confidence, with values greater than 0.7×10^{-7} and 1.4×10^{-7} N/m^3 shaded lightly and darkly over the ocean, respectively.

At lag 0, there is a subsynoptic-scale low at the surface in the STF region, centered around 27ºN, 145ºE, with anomalous southwesterly (northeasterly) winds to the northwest (southeast). The center of surface cyclonic curl is slightly shifted west of the low pressure center. The subsynoptic low is located next to a much larger, synoptic-scale high to the northwest centered around 35ºN, 135ºE. The high pressure is consistent with the downward motion seen there in the composite meridional sections (Fig. 2a). The anomalous northeasterly winds are part of this synoptic high. At the 500 hPa level, the subsynoptic low appears as a pressure trough extending southwestward from a low pressure center east of the surface synoptic high (Fig. 3).

The subsynoptic low can be traced back to the western edge of the STF around 23ºN, 130ºE at day -2 (We cannot trace this weak low further back in time.) Weak northerly winds are found on the western flank of the low, apparently as part of the synoptic high centered around 33ºN. There is no noticeable upper-level trough above the surface low, suggesting that the northerly winds of the synoptic high trigger an initial surface perturbation in the baroclinic zone over the STF.

Consistent with the result from the time-longitude diagrams, the subsynoptic low propagates eastward. From day -2 to +2, the low travels along 26ºN (the latitude of the STF) and intensifies along with the upper-level trough. During the course, the surface low is attached to the synoptic high to the north, which is a migratory midlatitude disturbance in the main storm track. The surface low weakens around day +4, and becomes unidentifiable by day +5. East of 160ºE, the STF still maintains large SST gradients, but the high-moisture tongue disappears with columnar water decreasing rapidly eastward (Fig. 2b). The decay of the surface low and high-moisture tongue is probably both due to low SST there (Fig. 2b) unfavorable for deep convection. Theoretical studies suggest that latent heating intensifies baroclinic instability.

The surface trough with cyclonic wind curls described in the present study appears to correspond to the so-called pre-Baiu/Meiyu front manifested as a cloud and rain band. It is one of the most remarkable events in the seasonal march of the East Asia summer monsoon. Using infrared satellite observations and surface weather maps, Kato and Kodama (1992) found a quasi-stationary cloud band in May along 25ºN before the onset of the Baiu season in Japan, which tends to form south of migratory anticyclones centered and propagating around 30º-40ºN. These characteristics are similar to our results. A similar cloud band is also found from Tanaka's (1992) long-term climatology of satellite cloud data. Wang and LinHo (2002) described a similar rain band based on long-term precipitation data. These studies, however, have not studied the underlying oceanic conditions and the STF in

particular. Our results suggest that the STF anchors this pre-Baiu/Meiyu cloud/rain band, a hypothesis that needs further investigations.

SUMMARY

The North Pacific subtropical front (STF) is a zone of high sea surface temperature (SST) gradients located around 25ºN in the western basin and most pronounced in spring. The STF's atmospheric effects are investigated using satellite observations and an atmospheric reanalysis. During April-May along the STF, surface wind stress curl turns weakly cyclonic in the general background of anticyclonic curls. Atmospheric column-integrated water vapor displays a pronounced meridional maximum along this surface trough, suggesting a deep vertical structure. Cyclonic wind curls occur intermittently at intervals of a few days along the STF in subsynoptic low pressure systems accompanying larger, synoptic highs in the main storm track to the north. In the subsynoptic surface lows, convective rain takes place, with deep upward motion moistening the entire troposphere. They display vertical structures characteristic of baroclinic instability, suggesting that they are triggered by the passage of synoptic migratory highs and grow on the baroclinicity anchored by the SST front. The surface trough with cyclonic wind curls along the STF appears to be related to a cloud/rain band associated with the so-called pre-Baiu/Meiyu front in May.

REFERENCES

Aoki, Y., T. Suga, and K. Hanawa, 2002: Subsurface subtropical fronts of the North Pacific as inherent boundaries in the ventilated thermocline. J. Phys. Oceanogr., 32, 2299-2311.

Hidaka, K, 1958: Computation of the wind stresses over the oceans. Records of Oceanographic Works in Japan, 4 (2), 77-123.

Kato, K., and Y. Kodama, 1992: Formation of the quasi-stationary Baiu front to the south of the Japan Islands in early May of 1979. J. Meteor. Soc. Japan, 70, 631-647.

Kobashi, F., H. Mitsudera, and S.-P. Xie, 2006: Three subtropical fronts in the North Pacific: Observational evidence for mode water-induced subsurface frontogenesis. J. Geophys. Res., 111, C09033, doi:10.1029/2006JC003479.

Kondo, J., 1975: Air-sea bulk transfer coefficients in diabatic conditions. Boundary-Layer Meteor., 9, 91-112.

Kubokawa, A., 1999: Ventilated thermocline strongly affected by a deep mixed layer: A theory for subtropical countercurrent. J. Phys. Oceanogr., 29, 1314-1333.

Kubokawa, A., and T. Inui, 1999: Subtropical countercurrent in an idealized ocean GCM. J. Phys. Oceanogr., 29, 1303-1313.

Onogi, K., J. Tsutsui, H. Koide, M. Sakamoto, S. Kobayashi, H. Hatsushika, T. Matsumoto, N. Yamazaki, H. Kamahori, K. Takahashi, S. Kadokura, K. Wada, K. Kato, R. Oyama, T. Ose, N. Mannoji and R. Taira, 2007: The JRA-25 Reanalysis. J. Meteor. Soc. Japan, 85, 369-432.

Takeuchi, K., 1984: Numerical study of the Subtropical Front and the Subtropical Countercurrent. J. Oceanogr. Soc. Japan, 40, 371-381.

Tanaka, M., 1992: Intraseasonal oscillation and the onset and retreat dates of the summer monsoon over East, Southeast Asia and the western Pacific region using GMS high cloud amount data. J. Meteor. Soc. Japan, 70, 613-629.

Uda, M., and K. Hasunuma, 1969: The eastward subtropical countercurrent in the western North Pacific Ocean. J. Oceanogr. Soc. Japan, 25, 201-210.

Wallace, J. M., T. P. Mitchell, and C. Deser, 1989: The influence of sea-surface temperature on surface wind in the eastern equatorial Pacific: seasonal and interannual variability. J. Clim., 2, 1492-1499.

Wang, B., and LinHo, 2002: Rainy season of the Asian-Pacific summer monsoon. J. Clim., 15, 386-398.

Xie, S.-P., 2004: Satellite observations of cool ocean-atmosphere interaction. Bull. Amer. Meteor. Soc., 85, 195-208.

Yoshida, K., and T. Kidokoro, 1967a: A subtropical countercurrent in the North Pacific - An eastward flow near the Subtropical Convergence. J. Oceanogr. Soc. Japan, 23, 88-91.

Yoshida, K., and T. Kidokoro, 1967b: A subtropical countercurrent (II) - A prediction of eastward flows at lower subtropical latitudes. J. Oceanogr. Soc. Japan, 23, 231-236.